Multiple scattering by a planar array of parallel dielectric cylinders

Steven J. Bever and Jan P. Allebach

The solution of the multiple-scattering problem for N parallel dielectric cylinders is considered for plane-wave illumination perpendicular to the cylinder axes. We describe a nonlinear programming approach to solve the multiple-scattering matrix for an arbitrary planar array of N parallel dielectric cylinders. To our knowledge, no calculations have been made previously for multiple scattering by more than two parallel dielectric cylinders. Numerical results for four abutting cylinders with end-on illumination demonstrate damping of internal resonance features similar to previously published results for two cylinders. Furthermore, we present numerical examples of scattering from eight unequally spaced, parallel dielectric cylinders with broadside illumination. Because of coupling between the cylinders, the incident energy is spread evenly between the intensity peaks behind the array of cylinders.

Key words: Multiple scattering, dielectric cylinders, iterative algorithms.

I. Introduction

In 1881 Lord Rayleigh[1] provided the solution of Maxwell's equations for the scattering of a normally incident plane wave by a single homogeneous dielectric cylinder of an arbitrary radius and refractive index. Since then, the scattering of a plane wave by clad, unclad, and inhomogeneous dielectric cylinders has been thoroughly investigated.[2–6] In addition, Presby[7] has shown that light scattered at right angles to the axis of an optical fiber can be used to measure its refractive index and diameter.

The solution of Maxwell's equations for the scattering of a plane wave by several cylinders is much more complex than the solution for a single cylinder. The added complexity is a consequence of the coupling between the cylinders. To solve for the scattered field, a set of equations that simultaneously enforce the boundary conditions at the surfaces of all the cylinders must be formulated. In 1952 Twersky[8] demonstrated that the scattering of a plane wave by an arbitary configuration of parallel cylinders can be expressed as an infinite sum of orders of scattering. The first order of scattering is the scattering from each cylinder owing to only the incident plane wave. The second order results from the scattering by each cylinder of the first order of scattering, and so on. In a later derivation,[9] Twersky demonstrated that the multiple-scattering coefficients can be generated from the corresponding single-scattering coefficients by using an iterative procedure.

In 1970 Olaofe[10] applied Twersky's iterative method to calculate the extinction and backscattering cross sections of two dielectric cylinders. He also mentioned in his paper that the linear equations involved could be solved by direct matrix inversion. Young and Bertrand[11] considered the scattering of an acoustic plane wave by two parallel, rigid cylinders, and they solved the resulting system of linear equations by using both the iterative procedure and direct matrix inversion. They found good agreement between their theoretical calculations and experimental results. However, no experimental results are available for scattering of light by two parallel dielectric cylinders. The primary difficulty in performing this experiment is establishing and maintaining parallelism between the two fibers while changing the separation between them.[12] Schlicht *et al.*[12] circumvented this problem to some extent by measuring the light scattered by a glass fiber that is parallel to and at varying distances from a highly reflective silver mirror. They showed that the multiple-scattering effects between a fiber and its mirror image are quite similar to those between two fibers.

In general, the numerical results for scattering by two cylinders presented in the literature are for cylinders that correspond to relatively small values of

Steven J. Bever is with the Department of Physics, Wabash College, Crawfordsville, Indiana 47933; Jan P. Allebach is with the School of Electrical Engineering, Purdue University, West Lafayette, Indiana 47907.

Received 23 July 1991.
0003-6935/92/183524-09$05.00/0.

the size parameter ka, where a is the radius, $k = 2\pi/\lambda$, and λ is the incident wavelength. The overall effect of a dielectric cylinder on an incident plane wave can be deduced from the value of ka. For example, when ka is much less than unity (the Rayleigh limit), the internal fields are uniformly distributed, and the external near field is only slightly modulated about the incident field value by a small scattered field. When ka is much greater than unity (the geometrical optics limit), the fiber can be modeled as a cylindrical thick lens. A line of focus is located behind the lens at a focal length that is dependent on the radius of the lens and the ratio between the index of refraction of the lens and that of the surrounding medium.[13] Benincasa *et al.*[13] made exact calculations of the near-field intensities and verified these results experimentally for a glass fiber with $ka = 488.5$. For ka between the Rayleigh and geometrical optics limits, complex internal and external fields are prevalent. For ka values in the range 39–51, calculations of the electric-field distributions within and around a dielectric cylinder have been performed.[14] Sharp internal resonances were observed when the ka value was in resonance with a natural mode of the dielectric cylinder. Such natural modes have been referred to as surface waves, since the internal fields are characterized by large peaks near the fiber surface. The solution of the multiple-scattering problem for two dielectric cylinders with ka in resonance with a natural mode was studied by Tsuei and Barber.[15] Yousif and Kohler[16] presented a general solution of the two-cylinder problem that is expressed in terms of Stokes vectors and Mueller matrices.

Returning to the model for the geometrical optics limit, we note that Machida *et al.*[17] showed that an optical-fiber sheet composed of a monolayer of abutting glass fibers of 25-μm-diameter ($ka = 124$) functions as a high-efficiency diffraction grating, which produces several tens of diffraction orders with uniform intensity. When a coherent plane wave is projected perpendicularly upon the fiber sheet, each fiber focuses its portion of the incident wave to a line just behind the grating. The far-field intensity pattern then consists of a multitude of uniformly spaced and uniform intensity points. Magnusson and Shin[18] analyzed the diffraction of plane waves by a periodic array of dielectric cylinders based on a complex transmittance approach. They assumed that the output field could be approximated by the product of the complex amplitude of the normally incident plane wave and the fiber grating transmittance function. Consequently, they found that the incident plane wave is diffracted into a spectrum of plane waves.

As described above, a common approach to calculating the field scattered by two parallel cylinders is to express the multiple-scattering linear equations in matrix form and then to solve the matrix expression for the multiple-scattering coefficients by Twersky's iterative method or by direct matrix inversion. However, for cylinders with ka values in resonance with natural modes, the iterative method diverges, and direct matrix inversion must be implemented.[15] In addition, the matrix-inversion approach fails as the matrices become ill-conditioned. The types of multiple-scattering problems for which an ill-conditioned matrix occurs are not well-defined.

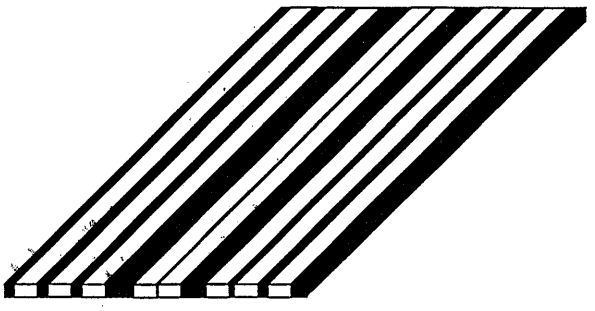

Fig. 1. Diffractive optical bar code that consists of transparent bars on an opaque background.

The results we present are part of a research effort to develop a new type of diffractive optical bar code. Two possible designs are shown in Figs. 1 and 2. A diffractive optical bar code composed of a number of transparent bars on an opaque background is shown in Fig. 1. The spacings between adjacent bars are chosen so that when the bar code is illuminated by a coherent plane wave, the first forward-scattered diffraction order represents a specified binary code. In Fig. 2 an alternate structure that we refer to as a modulated ribbon grating also seems well suited for use as a diffractive optical bar code. It is composed of a number of parallel equal-diameter transparent cylindrical fibers joined by flat sections of opaque or transparent material. For sufficiently large cylindrical fibers, each fiber focuses its portion of the incident wave to a line just behind the modulated ribbon grating. Thus the spacing between fibers is varied in the same manner as the spacing between bars in Fig. 1. And when illuminated by a plane wave, the resulting forward-scattered diffraction pattern is essentially the same as that observed with the structure in Fig. 1.

Here we extend Olaofe's multiple-scattering analysis for two cylinders to describe scattering from N identical, parallel, infinitely long circular cylinders. We describe a quadratic-programming approach to solve the associated multiple-scattering matrix expression. We present and compare results generated by a quadratic-programming algorithm for end-on

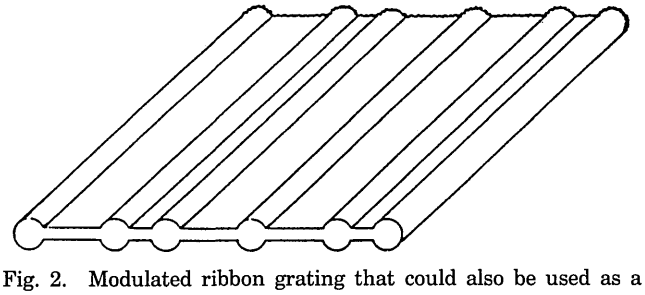

Fig. 2. Modulated ribbon grating that could also be used as a diffractive optical bar code.

illumination of four cylinders. To our knowledge, these are the first calculations for multiple scattering by more than two parallel dielectric cylinders. For broadside illumination we present numerical examples of scattering from eight unequally spaced parallel dielectric cylinders. Finally, we present calculations of the near-field scattering patterns for an infinite array of abutting cylinders.

II. Mathematical Formulation

Following Olaofe's[10] derivation, we wish to formulate the multiple-scattering problem for N identical, parallel, infinitely long circular cylinders C_p, with $p = 0, \ldots, N-1$. Each cylinder has a radius a, a uniform refractive index m, and a center located at the origin O_p, with $p = 0, \ldots, N-1$, of N parallel coordinate systems. The separation distance O_pO_q is denoted by d_{pq}, where $d_{pq} \geq 2a$, $\forall\, p \neq q$. We also denote by r_p, γ_p, and z the cylindrical polar coordinates with respect to the origin O_p, where it is assumed that $z_p = z$, $\forall p$. The polar axes O_pZ are the axes of the cylinders C_p, with $p = 0, \ldots, N-1$. The plane $z = 0$ is shown in Fig. 3.

As described by van de Hulst,[19] the total field can be expressed as the sum of transverse-magnetic (TM) and transverse-electric (TE) scalar potential functions. For the TM case the incident electric field is linearly polarized parallel to the cylinder axes. For the TE case the incident electric field is linearly polarized normal to the cylinder axes. Furthermore, the TM and TE scalar potential functions for the incident plane wave can be expressed with respect to the r_0, γ_0, z coordinate system as

$$u_0^{\text{inc}} = -i\,\frac{\exp(-i\omega t)}{k}\exp(i\rho_0\cos\gamma_0), \tag{1}$$

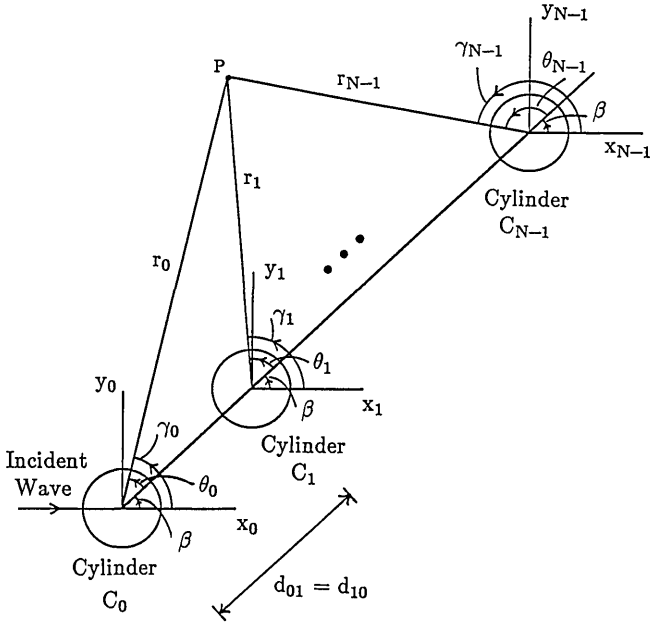

Fig. 3. Geometry of the problem. The axis of each cylinder is parallel to the z axis, which points out of the plane of the page.

$$u_0^{\text{inc}} = i\,\frac{\exp(-i\omega t)}{k}\exp(i\rho_0\cos\gamma_0), \tag{2}$$

where $\rho_0 = kr_0$, $k = 2\pi/\lambda$ is the wave number, ω is the angular frequency, and λ is the incident wavelength. Using the identity

$$\exp(i\rho\cos\gamma) = \sum_{n=-\infty}^{\infty} i^n J_n(\rho)\exp(-in\gamma) \tag{3}$$

and assuming that the incident plane wave impinges at an angle β with the line of centers C_0C_{N-1}, we can expand the incident wave in the coordinate system of cylinder C_p as

$$u_p^{\text{inc}} = -\frac{\exp(-i\omega t)}{k}\exp(i\delta_p\cos\beta) \times \sum_{n=-\infty}^{\infty} i^{n+1}J_n(\rho_p)\exp(-in\gamma_p), \tag{4}$$

$$v_p^{\text{inc}} = \frac{\exp(-i\omega t)}{k}\exp(i\delta_p\cos\beta) \times \sum_{n=-\infty}^{\infty} i^{n+1}J_n(\rho_p)\exp(-in\gamma_p). \tag{5}$$

Here $J_n(\rho_p)$ is the Bessel function of order n, $\delta_p = kd_{0p}$, and $\rho_p = kr_p$.

Similarly, the TM and the TE scattered wave potentials can be written in the form

$$u_p^{s} = \frac{\exp(-i\omega t)}{k}\sum_{n=-\infty}^{\infty} i^{n+1}\,{}_pb_n\,H_n(\rho_p)\exp(-in\gamma_p), \tag{6}$$

$$v_p^{s} = -\frac{\exp(-i\omega t)}{k}\sum_{n=-\infty}^{\infty} i^{n+1}\,{}_pa_n\,H_n(\rho_p)\exp(-in\gamma_p), \tag{7}$$

where ${}_pb_n$ and ${}_pa_n$ are the scattering coefficients to be determined by the boundary conditions. $H_n(\rho_p)$ is the Hankel function of the first kind, which corresponds to an $\exp(-i\omega t)$ time variation. Since the first-kind Hankel function is described by $(2/\pi\rho_p)^{1/2}\exp\{i[\rho_p - (2n+1)\pi/4]\}$ as $\rho_p \to \infty$, the radiation condition at infinity is satisfied.

Inside each cylinder the transmitted waves are

$$u_p^{\text{trans}} = \frac{\exp(-i\omega t)}{k}\sum_{n=-\infty}^{\infty} i^{n+1}\,{}_pd_n\,J_n(m\rho_p)\exp(-in\gamma_p). \tag{8}$$

$$v_p^{\text{trans}} = -\frac{\exp(-i\omega t)}{k}\sum_{n=-\infty}^{\infty} i^{n+1}\,{}_pc_n\,J_n(m\rho_p)\exp(-in\gamma_p), \tag{9}$$

where ${}_pd_n$ and ${}_pc_n$ are the transmission coefficients to be determined by the boundary conditions and m is the refractive index for the cylinder.

To enforce the boundary conditions that u and $\delta u/\delta r$ be continuous across the boundaries $r_p = a$, with $p = 0, \ldots, N-1$, the scattered field from the

qth cylinder must be expressed as an incident field on the pth cylinder. This is accomplished by means of the Graf addition theorem[20] as follows:

$$\exp(-in\theta_q)H_n(\rho_q) = \begin{cases} \sum_{l=-\infty}^{\infty} (-1)^l H_{n+l}(\delta_{pq})J_l(\rho_p)\exp(il\theta_p), & q < p, \\ (-1)^n \sum_{l=-\infty}^{\infty} H_{n+l}(\delta_{pq})J_l(\rho_p)\exp(il\theta_p), & q > p \end{cases} \tag{10}$$

where $\delta_{pq} = kd_{pq}$.

Applying the boundary conditions at $r_p = a$ and solving for the scattering coefficients of the pth cylinder leads to

$$ {}_pb_n = b_n\left[\exp(i\delta_p \cos\beta) + i^{n+1}\exp(in\beta)\sum_{q\neq p} {}_{pq}B_{-n}\right], \tag{11}$$

where

$$ {}_{pq}B_n = \begin{cases} \sum_{l=-\infty}^{\infty} (-1)^l i^{l+1} {}_qb_n \exp(-il\beta)H_{n+l}(\delta_{pq}), & p < q, \\ (-1)^n \sum_{l=-\infty}^{\infty} i^{l+1} {}_qb_n \exp(-il\beta)H_{n+l}(\delta_{pq}), & p > q \end{cases} \tag{12}$$

$$b_n = \frac{mJ_n(ka)J_n'(mka) - J_n'(ka)J_n(mka)}{mH_n(ka)J_n'(mka) - H_n'(ka)J_n(mka)} \tag{13}$$

are the single-cylinder scattering coefficients. The corresponding results for the TE scattering case are

$$ {}_pa_n = a_n\left[\exp(i\delta_p \cos\beta) + i^{n+1}\exp(in\beta)\sum_{q\neq p} {}_{pq}B_{-n}\right], \tag{14}$$

where

$$a_n = \frac{J_n(ka)J_n'(mka) - mJ_n'(ka)J_n(mka)}{H_n(ka)J_n'(mka) - mH_n'(ka)J_n(mka)} \tag{15}$$

and where ${}_qb_n$ is replaced by ${}_qa_n$ in Eq. (12).

Since Eq. (11) is linear, it can be written in matrix form as

$$\mathbf{L} = \mathbf{F} + \mathscr{C}\mathbf{L}, \tag{16}$$

where $\mathbf{L}$ is the vector of multiple-scattering coefficients, $\mathbf{F}$ is the vector of single-scattering coefficients, and the matrix $\mathscr{C}$ is called the coupling matrix, since it contains the multiple-scattering coupling information. For the TM case, $\mathbf{L}$ and $\mathbf{F}$ are defined as follows:

$$\mathbf{L} = [{}_0b_{-M}, \ldots, {}_0b_0, \ldots, {}_0b_M, \ldots, {}_{N-1}b_{-M}, \ldots, {}_{N-1}b_0, \ldots, {}_{N-1}b_M]^T, \tag{17}$$

$$\mathbf{F} = [b_{-M}\epsilon_0, \ldots, b_0\epsilon_0, \ldots, b_M\epsilon_0, \ldots, b_{-M}\epsilon_{N-1}, \ldots, b_0\epsilon_{N-1}, \ldots, b_M\epsilon_{N-1}]^T, \tag{18}$$

where $\epsilon_p = \exp(i\delta_p \cos\beta)$, and it is assumed that all summations have been truncated to $2M + 1$ elements. The entries of the coupling matrix $\mathscr{C}$ can be determined from Eqs. (11) and (12).

At this point the advantages of this approach are evident. The solution to Eq. (16) is given by

$$\mathbf{L} = (\mathscr{I} - \mathscr{C})^{-1}\mathbf{F}. \tag{19}$$

Thus the multiple-scattering problem for N cylinders reduces to a simple problem in linear algebra.

III. Numerical Solution Methods

Two common methods to solve Eq. (16) for the vector of multiple-scattering coefficients are matrix inversion and an iterative procedure.[10] From Eq. (19) it is clear that matrix inversion is the most direct approach. By substituting the expansion

$$(\mathscr{I} - \mathscr{C})^{-1} = \mathscr{I} + \mathscr{C} + \mathscr{C}^2 + \ldots \tag{20}$$

into Eq. (19), we find that

$$\mathbf{L} = \mathbf{F} + \mathscr{C}\mathbf{F} + \mathscr{C}^2\mathbf{F} + \ldots. \tag{21}$$

The steps of the iterative procedure can be deduced from Eq. (21). Starting with the initial estimate of the multiple-scattering coefficients $\mathbf{L} = \mathbf{F}$, we add coupling terms $\mathscr{C}\mathbf{F}$, $\mathscr{C}^2\mathbf{F}$, etc. to $\mathbf{L}$ until the desired convergence is obtained.

A third method of solving Eq. (16) uses a two-phase quadratic-programming algorithm[21] to find the minimum of the squared error

$$\epsilon_{\text{err}} = \frac{1}{2}\|\mathbf{F} - (\mathscr{I} - \mathscr{C})\mathbf{L}\|^2. \tag{22}$$

The algorithm is an iterative procedure that is designed to solve the constrained least-squares problem:

$$\underset{\mathbf{x}\in R^n}{\text{minimize}}\ G(\mathbf{x}) \tag{23}$$

subject to

$$\mathbf{l} \leq \begin{Bmatrix} \mathbf{x} \\ \mathscr{D}\mathbf{x} \end{Bmatrix} \leq \mathbf{u},$$

where

$$G(\mathbf{x}) = \tfrac{1}{2}\|\mathbf{b} - \mathscr{A}\mathbf{x}\|^2$$

and $\mathscr{D}$ is a constant coefficient matrix that represents linear constraints on the unknown variables $\mathbf{x}$. The vectors $\mathbf{l}$ and $\mathbf{u}$ provide the lower and upper bounds for the variables and the linear constraints. The two phases of the quadratic-programming method are: (1) finding an initial feasible point by minimizing the sum of feasibilities, and (2) minimizing the quadratic-objective function within the feasible region.[22]

For our problem we let $G(\mathbf{x}) = \epsilon_{err}$, where $\mathbf{x} = \mathbf{L}$, $\mathbf{b} = \mathbf{F}$, and $\mathscr{A} = (\mathscr{I} - \mathscr{C})$. The upper and lower bounds are set to infinity, and the general constraints matrix $\mathscr{D}$ is not used.

IV. Results

In Section II we considered the solution of the multiple-scattering problem for two polarizations of the normally incident wave: TM and TE. The calculation of the scattered field for a normally incident TM or TE wave can be performed by using the procedures described in Section III. Furthermore, for an arbitrary elliptically polarized wave the total scattered field can be calculated by summing the corresponding scattered vector fields. In this paper we consider the TM and TE wave cases separately.

For the TM incident-wave case, the first step in the numerical solution of the multiple-scattering problem for a planar array of dielectric cylinders is to generate the single-cylinder scattering coefficients in Eq. (13). These values multiplied by the appropriate factor $\exp(\delta_p \cos \beta)$ are the components of the vector $\mathbf{F}$. The entries of the coupling matrix $\mathscr{C}$ are then determined from Eqs. (11) and (12). For these calculations the Bessel functions of the first kind were found by using downward recursion. The Bessel functions of the second kind (the imaginary part of H_n^1) were found based on a special series expansion for small arguments. For moderate arguments an analytic continuation in the argument based on a Taylor series with special rational minimax approximations that provided starting values was employed. Finally, an asymptotic expansion was used for large arguments.[23] In Eqs. (6) and (7) the index n assumes values from $-\infty$ to ∞. To carry out the solution procedures discussed in Section III, the coefficient sequence for each cylinder must be truncated. For our investigation the number of single-scattering coefficients was selected by truncating the coefficient sequence after it had achieved a desired degree of convergence. The number of multiple-scattering coefficients for each cylinder was then set equal to this number. The steps outlined here were also used to find the numerical solution of the multiple-scattering problem for the TE case.

As we mentioned above, the matrix inversion method fails as the matrix $\mathscr{I} - \mathscr{C}$ becomes ill conditioned. However, during our studies of light scattering from dielectric cylinders, the coupling matrix became ill conditioned only when the specified degree of convergence of the single-scattering coefficient sequence was extremely small. For these cases the number of coefficients was large. Since the sequence of Bessel functions of the second kind diverges as $n \to \infty$, the matrix $\mathscr{I} - \mathscr{C}$ was ill conditioned. However, after the number of coefficients was reduced, the matrix-inversion method produced an acceptable solution.

For several of the results presented here, abutting cylinders with ka values in resonance with natural modes are considered. The iterative procedure diverged under these circumstances. Moreover, even though the squared errors for the results generated by quadratic programming were substantially lower than the squared errors for the results generated by matrix inversion, the corresponding intensity plots of scattering from the cylinders were virtually identical. Since in general the quadratic-programming algorithm produced solutions with lower squared error ϵ_{err}, all plots are for results generated by it.

A. Scattering from Four Cylinders with End-On Illumination

Owen *et al.*[14] have shown that a dramatic change occurs in the internal field of a dielectric cylinder as the size parameter of the cylinder is varied. An interesting case for which coupling between two cylinders with ka in resonance with a natural mode was studied by Tsuei and Barber.[15] At resonance the internal intensity of an isolated cylinder is an order of magnitude greater than the nonresonant case, and the intensity is concentrated at the surface of the cylinder. They found that for two abutting cylinders the resonant nature of the cylinders was damped.

For end-on illumination, Figs. 4 and 5 show the intensity patterns within and around four abutting cylinders with ka in resonance with a natural mode for TM and TE polarizations, respectively. Previous research[14] for an isolated dielectric cylinder with an index of refraction of 1.53 showed that a third-order resonance of mode 53 occurs when the size parameter is 45.329 for TM illumination. A third-order reso-

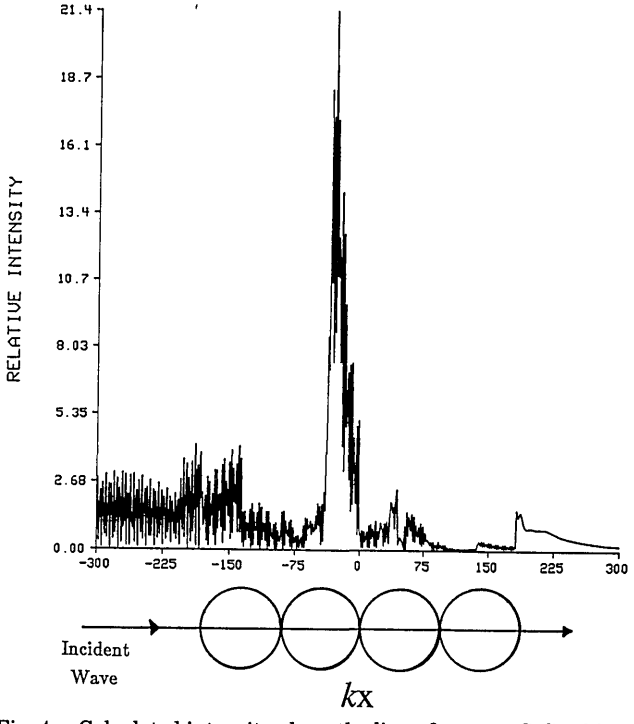

Fig. 4. Calculated intensity along the line of centers C_0C_3 of four abutting infinite cylinders with ka in resonance with a natural mode for end-on illumination and TM polarization ($ka = 45.329$, $m = 1.530$, and $\delta = 2ka = 90.658$). The location of each cylinder is shown by a circle below the kx axis.

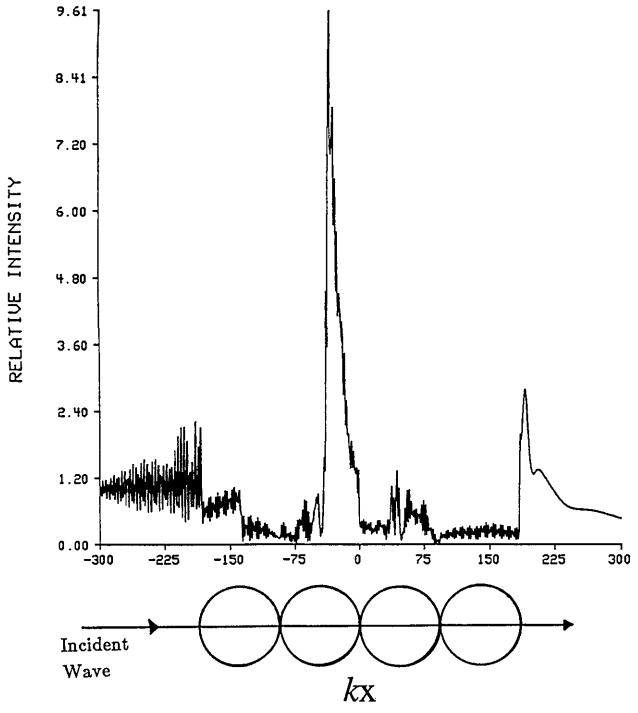

Fig. 5. As in Fig. 4 but with TE polarization (ka = 45.726, m = 1.530, and $\delta = 2ka$ = 91.452).

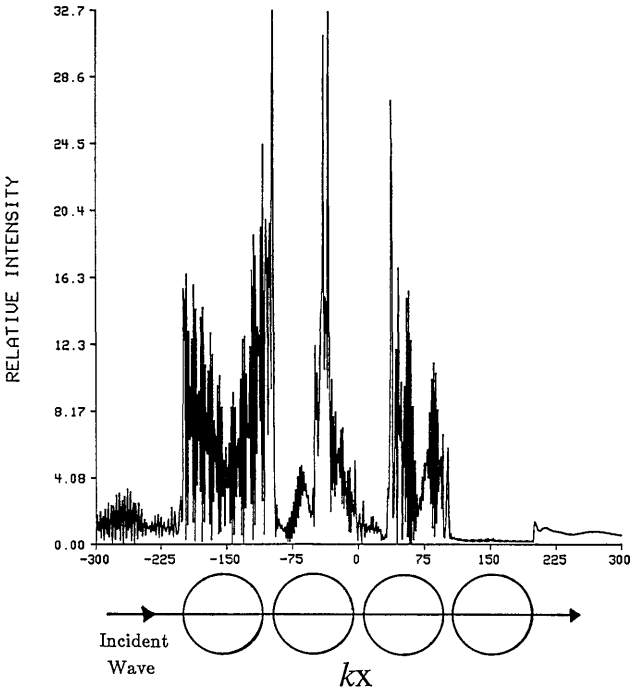

Fig. 6. As in Fig. 4 but with TM polarization (ka = 45.239, m = 1.530, and δ = 101.99).

nance of mode 53 also occurs when the size parameter is 45.726 for TE illumination.[14] The intensity patterns in Figs. 4 and 5 indicate that damping of the resonant nature of the cylinders occurs for four abutting cylinders. The internal and total-external intensities are given by $|E^{\text{trans}}|^2$ and $|E^{\text{inc}} + \Sigma_{p=0}^{3} {}_{p}E^{s}|^2$. For our calculations the incident intensity has been set to unity. As a result of the symmetry about the direction of propagation for end-on illumination ($\beta = 0°$) and the fact that the cylinders are uniformly spaced, the multiple-scattering coefficients with positive indices are the same as those with negative indices. Therefore the number of entries in the coupling matrix $\mathscr{C}$ can be reduced by approximately a factor of 4. As expected, large-scale similarities are seen between the scattered intensity patterns for the two polarizations. However, as found by Abushagur and George[24] for a single cylinder, the fine structures of the scattered fields differ significantly.

Figures 6–9 show that the resonant character of the cylinders is no longer damped when the cylinders in Figs. 4 and 5 are moved apart in the presence of end-on illumination. However, instead of the internal intensity of the first cylinder concentrating at the surface as previously shown for the two-cylinder TM case,[15] Fig. 6 shows an intensity distribution throughout the first cylinder. For the TE case the results in Fig. 7 indicate that the damping effect is negligible for the first cylinder since large peaks are present near the fiber surface. The resonant nature of the fourth cylinder is not strikingly apparent in Figs. 6 and 7, possibly as a result of this cylinder being in the shadow of the first three cylinders. Figures 8 and 9 demonstrate the decrease in coupling between the cylinders as they are separated for the TM and TE cases, respectively. Once again, shadow effects are visible in Figs. 8 and 9.

B. Scattering from Eight Unequally Spaced Cylinders with Broadside Illumination

Scattering of a TM wave for broadside illumination ($\beta = 90°$) from eight unequally spaced, parallel dielec-

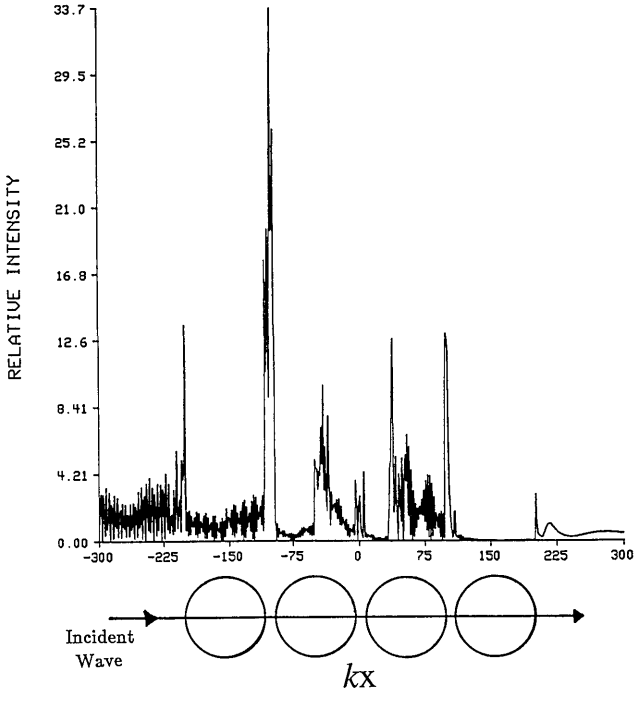

Fig. 7. As in Fig. 4 but with TE polarization (ka = 45.726, m = 1.530, and δ = 102.88).

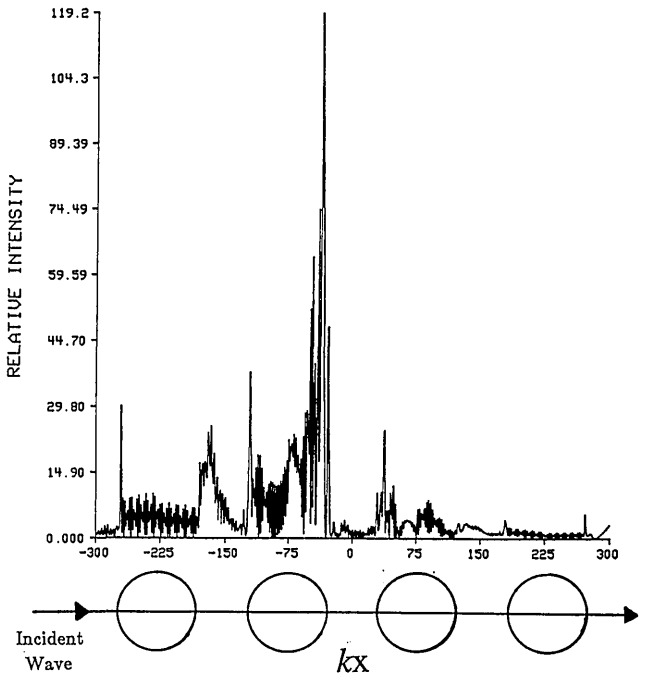

Fig. 8. As in Fig. 4 but with TM polarization (ka = 45.329, m = 1.530, and δ = 150.00).

tric cylinders of radius 2.52 μm (ka = 25) is shown in Fig. 10. The relative intensity for each of the peaks is given. The specular reflection behind the illuminated side of each cylinder gives a complicated pattern that results from the interaction of the scattered and incident fields. The strong focused intensity peak on the shadow side of each cylinder demonstrates the focusing ability of the cylinders. The corresponding intensity plot for the TE case is shown

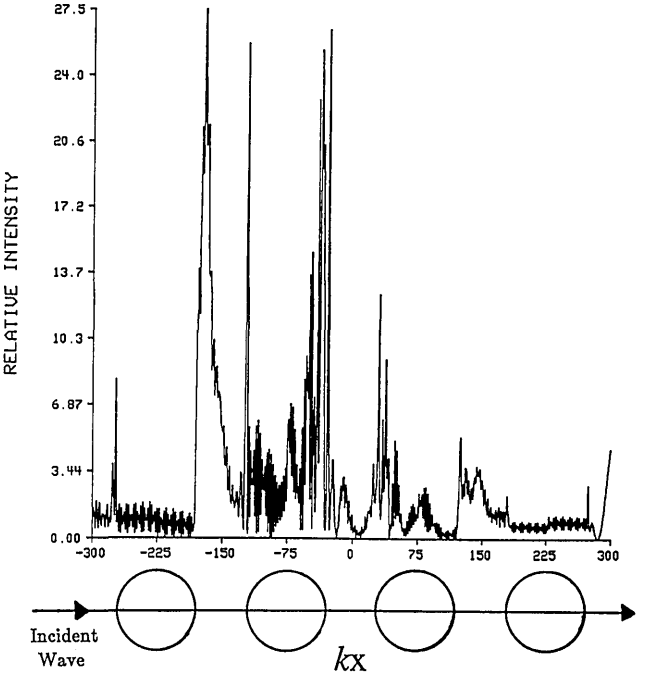

Fig. 9. As in Fig. 4 but with TE polarization (ka = 45.726, m = 1.530, and δ = 151.31).

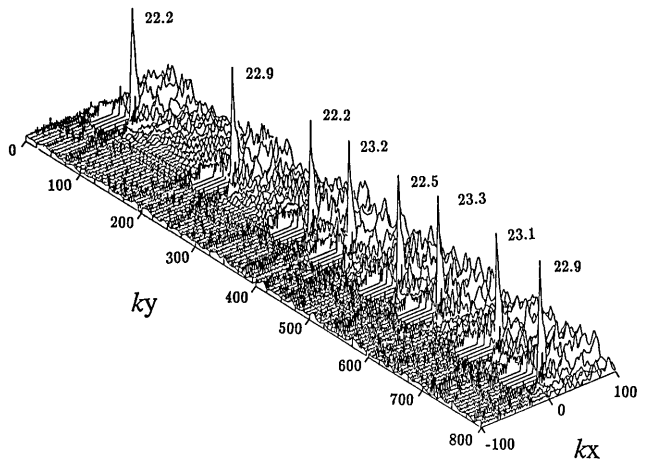

Fig. 10. Near-field intensity distribution over the xy plane of eight unequally spaced, parallel dielectric cylinders for a = 2.52 μm with ka = 25 and m = 1.530 for a TM-polarized wave incident from the left. The internal intensity of each cylinder is set equal to zero.

in Fig. 11. The intensity plot for the TM case that results from using the isolated-cylinder coefficients instead of the multiple-scattering coefficients is displayed in Fig. 12. Comparing Figs. 10 and 12, we see the effects of coupling even for broadside illumination. The coupling between the eight cylinders contributes both constructively and destructively to the intensity peaks. Consequently, the incident energy is spread evenly between the intensity peaks.

C. Scattering from an Infinite Array of Abutting Cylinders

The intensity distribution on the shadow side of a single fiber from an optical-fiber sheet composed of an infinite number of abutting glass fibers with diameter 25 μm (ka = 124) for TM illumination is shown in Fig. 13. Since the fiber sheet is infinite in extent, the multiple-scattering coefficients for each fiber are identical and the coefficients with positive indices are the same as those with negative indices. During our investigation, we observed that contributions from fibers more than 10 diameters away added little to the scattered field by a fiber of the array. Thus, for Fig. 13, contributions from fibers more than 10 diameters

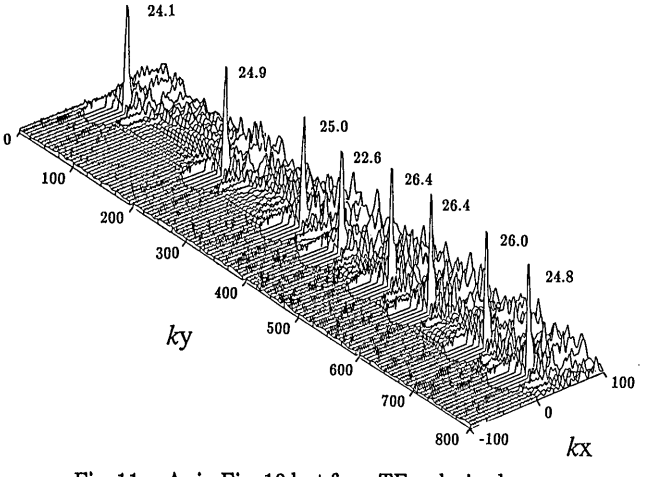

Fig. 11. As in Fig. 10 but for a TE-polarized wave.

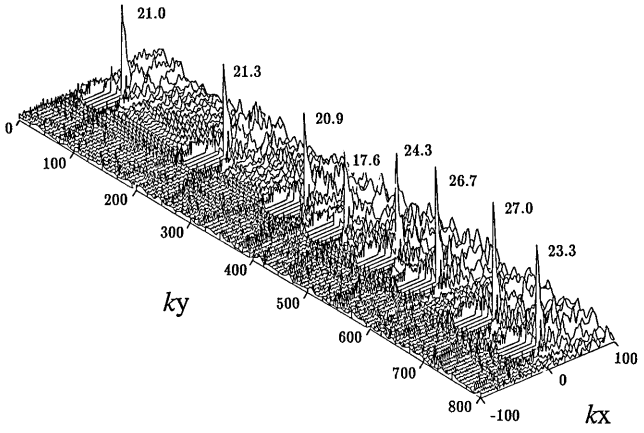

Fig. 12. As in Fig. 10 except that the isolated-cylinder coefficients were used instead of the multiple-scattering coefficients.

away were ignored. Furthermore, we assumed that the kz axis was the axis of the infinitely long fiber. On the shadow side of the fiber a pair of intensity peaks along the kx axis and two clusters of intensity peaks near the surface of the fiber are observed in Fig. 13. This result disagrees with the single intensity peak of the cylindrical lens model. Moreover, the intensity region composed of these peaks is relatively large in comparison to the fiber width. For a slit grating the number of evenly spaced, uniform intensity peaks in the far-field intensity pattern decreases as the slit width is increased. In the same manner the number of uniform intensity peaks in the intensity pattern for a fiber grating decreases as the width of the intensity peaks increases. Therefore significant roll-off of the intensity peaks in the diffraction pattern will be observed for a fiber sheet composed of glass fibers with a diameter of 25 μm. An exact method of calculating the far-field intensity pattern for a fiber grating is currently under development.

VI. Conclusions

Following a method originally developed by Olaofe, we have shown that the multiple-scattering problem for N cylinders reduces to a simple problem in linear algebra. For cylinders with size parameter ka in resonance with a natural mode both direct matrix inversion and a quadratic-programming algorithm may be used to calculate the multiple-scattering coefficients. Since in general the squared error was substantially lower for solutions generated by the quadratic-programming algorithm, all results were generated by this method. We have presented calculations for multiple scattering by four cylinders with end-on illumination. The results demonstrated damping of internal resonance features similar to previously published results for two cylinders. Furthermore, we have presented results for scattering from eight unequally spaced, parallel dielectric cylinders with broadside illumination. Because of coupling between the cylinders, the incident energy was spread evenly between the intensity peaks behind the array of cylinders. Finally, the near-field intensity pattern for an infinite array of abutting cylinders was shown. On the shadow side of a cylinder from the array a pair of intensity peaks along the kx axis and two clusters of intensity peaks near the surface of the cylinder were observed instead of the single intensity peak that is predicted by the cylindrical lens model. Considerably further research is needed to calculate the exact far-field intensity pattern for an infinite array of abutting cylinders.

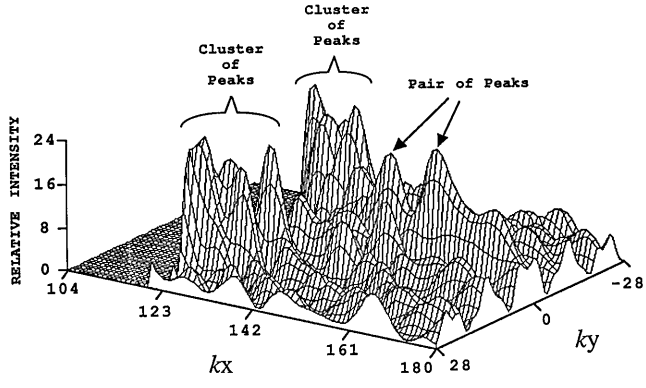

Fig. 13. Near-field intensity distribution over the xy plane on the shadow side of a single fiber from an optical-fiber sheet for $a = 12.5$ μm with $ka = 124$ and $m = 1.530$ for a TM-polarized wave incident from the left. The internal intensity of the fiber is set equal to zero.

References

1. Lord Rayleigh, "On the electromagnetic theory of light," Philos. Mag. **12,** 81–101 (1881).
2. J. R. Wait, "Scattering of a plane wave from a circular dielectric cylinder at oblique incidence," Can. J. Phys. **33,** 189–195 (1955).
3. L. B. Evans, J. C. Chen, and S. W. Churchill, "Scattering of electromagnetic radiation by infinitely long, hollow, and coated cylinders," J. Opt. Soc. Am. **54,** 1004–1007 (1964).
4. W. A. Farone and C. W. Querfeld, "Electromagnetic scattering from radially inhomogeneous infinite cylinders at oblique incidence," J. Opt. Soc. Am. **56,** 476–491 (1966).
5. D. D. Cooke and M. Kerker, "Light scattering from long thin glass cylinders at oblique incidence," J. Opt. Soc. Am. **59,** 43–49 (1969).
6. C. Saekeang and P. L. Chu, "Backscattering of light from optical fibers with arbitrary refractive-index distributions: uniform approximation approach," J. Opt. Soc. Am. **68,** 1298–1305 (1978).
7. H. M. Presby, "Refractive index and diameter measurements of unclad optical fibers," J. Opt. Soc. Am. **64,** 280–284 (1974).
8. V. Twersky, "Multiple scattering of radiation by an arbitrary planar configuration of parallel cylinders," J. Acoust. Soc. Am. **24,** 42–46 (1952).
9. V. Twersky, "Scattering of waves by two objects," in *Electromagnetic Waves,* R. E. Langer, ed. (University of Wisconsin, Madison, Wisc., 1962), pp. 361–389.
10. G. O. Olaofe, "Scattering by two cylinders," Radio Sci. **5,** 1351–1360 (1970).
11. J. W. Young and J. C. Bertrand, "Multiple scattering by two cylinders," J. Acoust. Soc. Am. **58,** 1190–1195 (1975).
12. B. Schlicht, K. F. Wall, and R. K. Chang, "Light scattering by two parallel glass fibers," J. Opt. Soc. Am. A **4,** 800–809 (1987).
13. D. S. Benincasa, P. W. Barber, J.-Z. Zhang, W.-F. Hsieh, and R. K. Chang, "Spatial distribution of the internal and near-

field intensities of large cylindrical and spherical scatterers," Appl. Opt. **26,** 1348–1356 (1987).
14. J. F. Owen, R. K. Chang, and P. W. Barber, "Internal electric field distributions of a dielectric cylinder at resonant wavelengths," J. Opt. Soc. Am. **6,** 540–542 (1981).
15. T.-G. Tsuei and P. W. Barber, "Multiple scattering by two parallel dielectric cylinders," Appl. Opt. **27,** 3375–3381 (1988).
16. H. A. Yousif and S. Kohler, "Scattering by two penetrable cylinders at oblique incidence. I. The analytical solution," J. Opt. Soc. Am. A **5,** 1085–1096 (1988).
17. H. Machida, J. Nitta, A. Seko, and H. Kobayashi, "High-efficiency fiber grating for producing multiple beams of uniform intensity," Appl. Opt. **23,** 330–332 (1984).
18. R. Magnusson and D. Shin, "Diffraction by periodic arrays of dielectric cylinders," J. Opt. Soc. Am. A **6,** 412–414 (1989).
19. H. C. van de Hulst, *Light Scattering by Small Particles* (Wiley, New York, 1957).
20. M. A. Abramowitz and I. A. Stegun, eds., *Handbook of Mathematical Functions* (National Bureau of Standards, Washington, D.C., 1964), Chap. 9, Sec. 9.1.79, p. 363.
21. P. E. Gill, S. J. Hammarling, W. Murray, M. A. Saunders, and M. H. Wright, "User's guide for LSSOL (version 1.0): a FORTRAN package for constrained linear least-squares and convex quadratic programming," SOL 86-1 (Department of Operations Research, Stanford University, Stanford, Calif., 1986).
22. P. E. Gill, W. Murray, and M. H. Wright, *Practical Optimization* (Academic, New York, 1981).
23. International Mathematics and Statistics Libraries, "IMSL edition 10.0" (IMSL, Inc., Houston, Tex., 1988).
24. M. A. Abushagur and N. George, "Polarization and wavelength effects on the scattering from dielectric cylinders," Appl. Opt. **27,** 3375–3381 (1988).